

Irradiation of the prostate and pelvic lymph nodes with an adaptive algorithm

A. B. Hwang^{a)} and J. Chen

Department of Radiation Oncology, University of California San Francisco, 1600 Divisadero Street, San Francisco, California 94143

T. B. Nguyen

Prowess Inc., Concord, California 94520

A. G. Gottschalk, M. R. Roach III, and J. Pouliot

Department of Radiation Oncology, University of California San Francisco, 1600 Divisadero Street, San Francisco, California 94143

(Received 4 March 2011; revised 1 January 2012; accepted for publication 9 January 2012; published 6 February 2012)

Purpose: The simultaneous treatment of pelvic lymph nodes and the prostate in radiotherapy for prostate cancer is complicated by the independent motion of these two target volumes. In this work, the authors study a method to adapt intensity modulated radiation therapy (IMRT) treatment plans so as to compensate for this motion by adaptively morphing the multileaf collimator apertures and adjusting the segment weights.

Methods: The study used CT images, tumor volumes, and normal tissue contours from patients treated in our institution. An IMRT treatment plan was then created using direct aperture optimization to deliver 45 Gy to the pelvic lymph nodes and 50 Gy to the prostate and seminal vesicles. The prostate target volume was then shifted in either the anterior-posterior direction or in the superior-inferior direction. The treatment plan was adapted by adjusting the aperture shapes with or without re-optimizing the segment weighting. The dose to the target volumes was then determined for the adapted plan.

Results: Without compensation for prostate motion, 1 cm shifts of the prostate resulted in an average decrease of 14% in D-95%. If the isocenter is simply shifted to match the prostate motion, the prostate receives the correct dose but the pelvic lymph nodes are underdosed by $14\% \pm 6\%$. The use of adaptive morphing (with or without segment weight optimization) reduces the average change in D-95% to less than 5% for both the pelvic lymph nodes and the prostate.

Conclusions: Adaptive morphing with and without segment weight optimization can be used to compensate for the independent motion of the prostate and lymph nodes when combined with daily imaging or other methods to track the prostate motion. This method allows the delivery of the correct dose to both the prostate and lymph nodes with only small changes to the dose delivered to the target volumes. © 2012 American Association of Physicists in Medicine. [DOI: 10.1118/1.3679859]

Key words: adaptive radiotherapy, prostate cancer, image guided therapy, prostate therapy, treatment planning

I. INTRODUCTION

Although the prophylactic irradiation of lymph nodes is routine practice for many cancer sites, the role of pelvic lymph node irradiation in the treatment of localized prostate cancer is still somewhat controversial despite data showing a progression free survival benefit.¹ Intensity modulated radiation therapy (IMRT) has been shown to be superior to 3D-conformal radiotherapy (3D-CRT) for the treatment of prostate cancer.^{2,3} The advantages of IMRT are believed to be even greater when the pelvic lymph nodes are treated in addition to the prostate gland itself.^{4,5} These advantages result from the ability to create more conformal dose distributions that minimize dose to normal structures (*e.g.*, bladder, rectum, and bowel) when using IMRT.

One difficulty in the use of IMRT results from interfraction motion of the prostate negating the advantages of conformal dose distributions. Due to differences in bladder

and rectum filling the position of the prostate can vary up to 1.5 cm from day to day.⁶ A common approach to compensate for this motion is to shift the isocenter to track the daily change in prostate position.⁷ Although shifting the isocenter can alter the source to skin distances (SSDs) and the effective depth of the target volume (*i.e.*, prostate), the resulting dosimetric impact on the prostate has been shown to be insignificant.⁸

Although the prostate is highly mobile, the pelvic lymph nodes are in close proximity to vascular structures which are presumably fixed with respect to bony anatomy.⁹ Thus, the lymph nodes and the prostate move independently and shifting the isocenter to compensate for prostate motion may reduce the dose to the pelvic lymph nodes, particularly in highly conformal IMRT treatment plans. Therefore, to deliver IMRT treatments simultaneously to the prostate and pelvic lymph nodes while using tight margins requires the ability to target fixed and mobile tumor volumes at the same time.

The purpose of this study is to demonstrate an adaptive algorithm¹⁰ (RealART) to compensate for the independent motion of the prostate and pelvic lymph nodes. This algorithm is applied to an IMRT plan created using direct aperture optimization (DAO). It first adapts the individual MLC apertures (segments) and then optionally re-optimizes the segment weighting. To evaluate the potential use of this algorithm, we test the algorithm using data simulating various shifts in prostate position relative to the pelvic lymph nodes.

II. MATERIALS AND METHODS

We used the treatment planning CT scans and contours from five patients treated for prostate cancer at UCSF. IMRT treatment plans were created using the Prowess Panther treatment planning system (version 5.00, Prowess, Inc., Concord, CA) to deliver 50 Gy in 25 fractions to the expanded prostate (prostate + 2 mm margin) and seminal vesicles. Patient 5 was postprostatectomy, therefore the target volume was comprised of the prostate bed and lymph nodes and the seminal vesicles were not treated. The plans also delivered 45 Gy to the pelvic lymph nodes (1.8 Gy/fx). This is a common fractionation scheme used in our institution that is usually followed with a boost to the prostate delivered using either external beam radiotherapy or brachytherapy. The plans were created using 6 MV beams from a Siemens Oncor linear accelerator and used a total of seven beam angles and were designed to minimize dose to normal tissues. Plans were normalized such that 95% of the target volumes received the prescribed dose. Treatment plan characteristics for the five patients are summarized in Table I.

To test the adaptive algorithm, we created new patient models which contained the clinical target volumes. However, the prostate and seminal vesicles were shifted by 0.3, 0.6, 1.0 cm in the anterior, posterior, superior, or inferior direction in the new patient models to simulate prostate motion. A total of four

treatment plans were applied to each patient model. The first treatment plan was the original plan without any compensation for prostate motion. The second treatment plan was the original treatment plan with the isocenter shifted to match the prostate motion and is identified as the isoshift method. The third approach was to copy the original treatment plan to the original isocenter, but to “morph” the IMRT apertures using the aperture morphing feature of the treatment planning system. This morphing algorithm takes the MLC leaves and attempts to maintain their positions relative to the outline of the target volume, which in this study consisted of the union of the target volumes (prostate, seminal vesicles, and pelvic lymph nodes). The final approach takes the morphed apertures and applies segment weight re-optimization. This method re-optimizes the plan by adjusting the segment weights using the original plan objectives for the target structures, specifically the CTV (expanded prostate), seminal vesicles, and the lymph nodes. Specifically, the objectives for segment weight optimization consisted of minimum dose, maximum dose, and dose-volume objective (D-95%) objectives for the target structures.

In addition, we also copied the bladder and rectum contours onto the CT. These were shifted along with the prostate and seminal vesicles. Although these structures deform and do not shift rigidly, we used a simple rigid model as a first order approximation. By making the assumption that the high dose regions in the organs at risk (OAR) are found near the prostate-OAR interface, we can use the translated structures to study the bladder and rectum dose. Constraints on normal structures (*e.g.*, rectum and bladder) were not used for segment weight optimization in this study.

After the dose has been calculated, DVH data are extracted for the prostate (without expansion), seminal vesicles, and nodes for each plan. Parameters included D-95% (dose to 95% of the volume) and maximum dose. Changes in the various dosimetric parameters relative to the values in the original plan were then calculated.

Finally, we performed a simulation to determine the cumulative dose that would be obtained over multiple fractions. Using the CT data set, contours, and treatment plan for one patient (Patient 3), we simulated prostate motion using the daily prostate shifts measured from a patient treated at our institution. These prostate shifts were determined using a double registration method that first removed set-up error through alignment of bony anatomy and then measured prostate motion via alignment of marker seeds implanted in the prostate.¹¹ For each fraction, each of the four different adaptive methods was simulated. The dose matrices from each fraction were exported and combined using MATLAB (Mathworks, Natick, MA). We simulated a total of 18 fractions based on the available prostate shift data.

III. RESULTS

The results for 1 cm simulated shifts in prostate position are summarized in Fig. 1. The data show that without any correction for prostate motion, the dose to the prostate (D-95%) decreases an average of $14\% \pm 8\%$ when the prostate moves 1 cm in any direction. When the isocenter is

TABLE I. Treatment plan characteristics.

	Pt. #1	Pt. #2	Pt. #3	Pt. #4	Pt. #5
Prostate volume (cm ³)	24.9	33.3	21.8	23.9	68.7
Expanded prostate					
D-1cc (cGy)	5596	5318	5654	5637	5485
D95% (cGy)	4928	4898	4983	5039	5003
Lymph nodes					
D-1cc (cGy)	5570	5616	5504	5489	5240
D95% (cGy)	4454	4496	4483	4517	4488
Seminal vesicles					
D-1cc (cGy)	5388	5257	5508	5409	—
D95% (cGy)	5053	4959	4893	4897	—
Rectum					
D-1cc (cGy)	4718	4848	5080	5080	4872
V30Gy (%)	43.0	51.6	54.6	45.4	48.9
Bladder					
D-1cc (cGy)	5368	5216	5321	5165	5227
V30Gy (%)	48.8	53.6	69.1	61.1	67.3

Note: D-1cc: highest dose received by 1 cm³ of the structure. V30Gy: percent volume of a structure receiving 30 Gy or more.

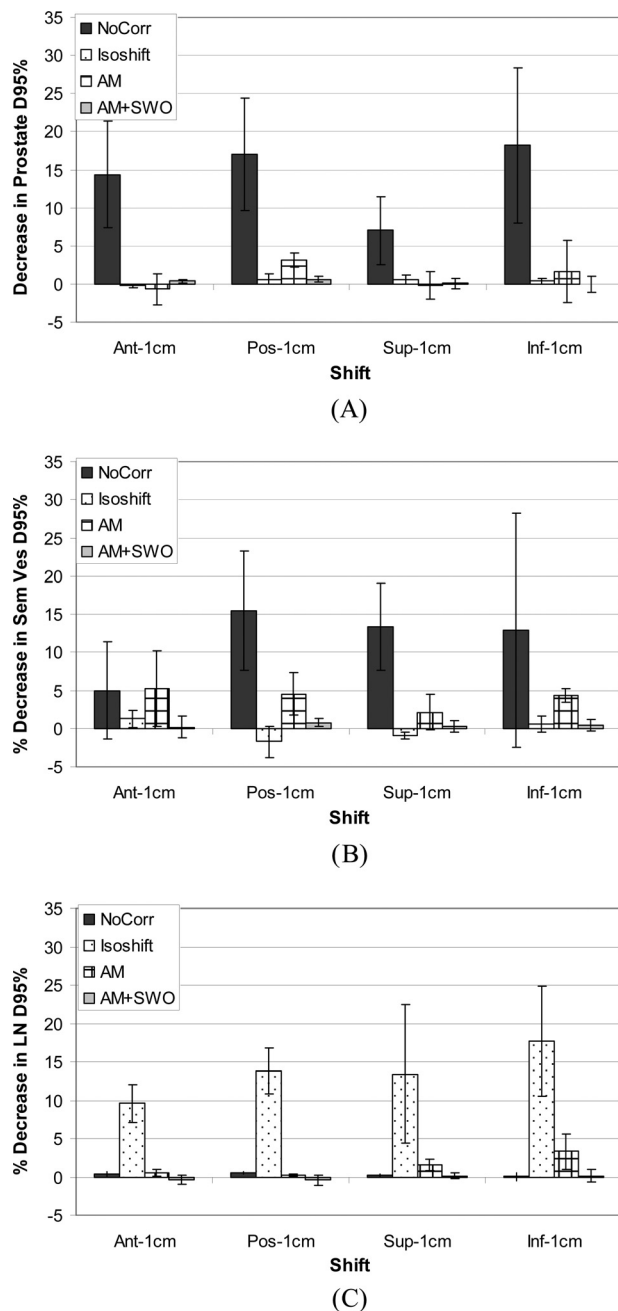


FIG. 1. (a) Decrease in D-95% to the prostate for different changes in prostate position. Results for 4 different correction strategies are compared. (b) Decrease in D-95% to the seminal vesicles for different changes in prostate position. (c) Decrease in D-95% to the lymph nodes for different changes in prostate position. Error bars represent the standard deviation.

shifted to match the prostate motion, the prostate receives the prescribed dose with only negligible changes due to changes in SSD and/or effective depth. However, the dose to the lymph nodes is reduced (decrease in D-95% by $14\% \pm 6\%$). When the adaptive morphing strategy is employed, the average change in D-95% is less than 5% for all three target volumes (prostate, seminal vesicles, and lymph nodes). Adding segment weight optimization further decreases changes in the dose delivered to the target volumes (*i.e.*, improves coverage), particularly for the seminal vesicles. These results obviously apply only to a single fraction and the cumulative effect on

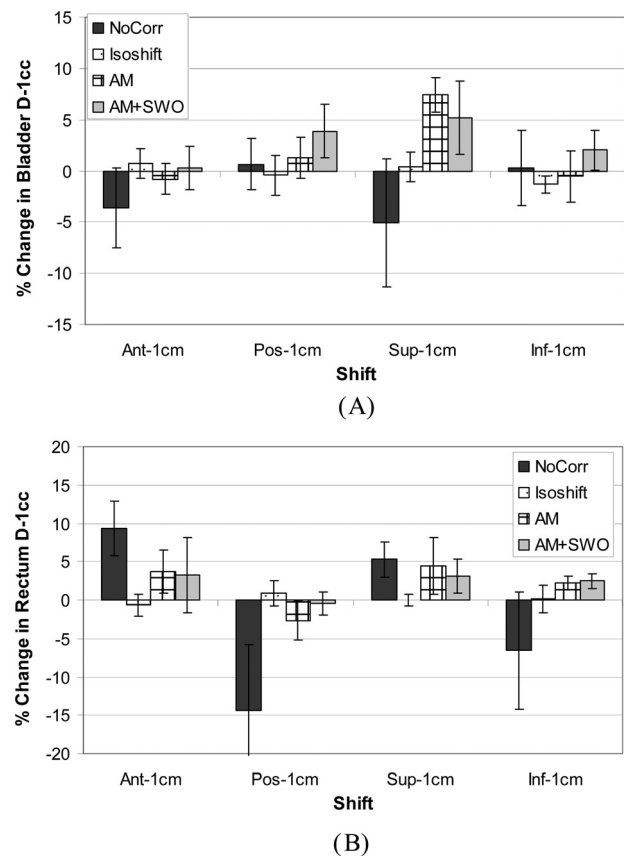


FIG. 2. Change in D-1cc received by (a) bladder and (b) rectum for different changes in prostate position and with different adaptive strategies.

the entire treatment depends on the frequency and magnitude of the prostate shifts relative to the bony anatomy over the whole course of treatment.

The dose to the bladder and rectum for 1 cm shifts are plotted in Fig. 2. As expected, the data show that without corrections, certain movements of the prostate will increase the dose to the OAR. For example, an anterior movement of the prostate will cause the rectum to receive the full prescription dose. Likewise, the same motion will decrease the dose to the bladder. By shifting the isocenter with the prostate, the changes to the bladder and rectum are minimal. Aperture morphing with or without segment weight optimization result in small changes (less than 5% in most cases) to the bladder and rectum dose D-1 cc values.

Figure 3 plots the dose to the prostate (D-95%) as a function of the magnitude of the prostate shift. The effects of shifts in different directions are averaged together. The results show that all three adaptive strategies (isocenter shifting, adaptive morphing, and adaptive morphing with segment weight optimization) provide adequate prostate coverage. Without correction, a prostate movement of 6 mm results in an average decrease in prostate dose of approximately 5%. This decrease in dose varies from patient to patient, as well as with the direction of motion. Posterior prostate shifts result in greater decreases in dose coverage, due to steeper dose gradients in the posterior direction. The dose to the lymph nodes as a function of motion is plotted in Fig. 4. Shifting the isocenter to compensate for prostate

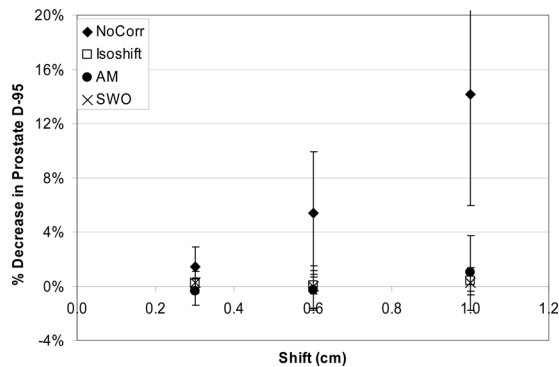


FIG. 3. Decrease in prostate D-95% as a function of motion (averaged over all patients and directions) for different adaptive strategies.

motion will reduce dose to the lymph nodes, with a 6 mm motion resulting in D-95% decreasing by an average of 4.6%. Aperture morphing produces an average D-95% for the lymph nodes within a few percent of the original plan. The addition of segment weight re-optimization further improves target coverage, with greater improvements seen for the larger 1 cm prostate shifts.

The prostate shifts used in our simulation of a single patient treatment are shown in Fig. 5. The root-mean-square prostate motion in the left-right, anterior-posterior, and superior-inferior directions are 1.5, 2.7, and 4.7 mm, respectively. The dosimetric results for the simulated treatment course are shown in Table II. For this particular patient, treatment without prostate motion compensation results in only minor changes to the prostate and lymph node doses but a 5% reduction in dose to the seminal vesicles. Isocenter shifting maintains the dose to the prostate and seminal vesicles but results in 5% reduction in dose to the lymph nodes. Adaptive morphing with or without segment weight optimization results in consistent or improved dose coverage to all three target structures.

IV. DISCUSSION

In this work, we have demonstrated a method that can potentially be used to compensate for the independent motion of the pelvic lymph nodes and the prostate. Daily imaging is used to first eliminate set-up error and then to adapt the plan to compensate for the inter-fraction motion of

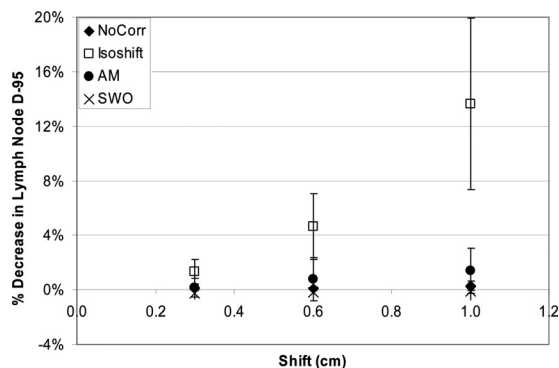


FIG. 4. Change in pelvic lymph node D-95% as a function of motion (averaged over all patients and directions) for different adaptive strategies.

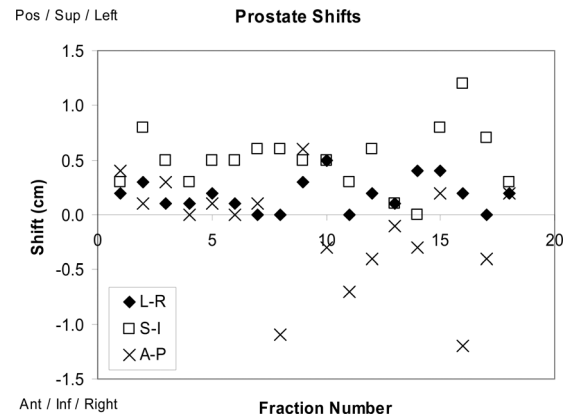


FIG. 5. Daily prostate shifts used in the treatment simulation. The prostate motions along the three axes are plotted for each fraction. The root-mean-square shifts are 1.5, 2.7, and 4.7 mm in the left-right (L-R), superior-inferior (S-I), and anterior-posterior (A-P) directions, respectively.

the prostate. Aperture morphing with or without segment weight re-optimization was able to maintain good dose coverage for both the prostate/seminal vesicles and lymph nodes volumes for internal prostate motion of up to 1 cm. We studied shifts up to 1 cm due to previously published data that suggest that the daily prostate motion will be less than 1 cm for the majority of treatments.^{6,7,12,13} With this large shift and tight margins (2 mm), we generated challenging test cases for the algorithm. Although we only studied translations along the anterior-posterior and caudal-cranial axes, the adaptive morphing and segment weight optimization can easily be applied to prostate motion in arbitrary directions. The method could also potentially correct for rotation or deformation of the target volumes.

One potential problem with segment weight optimization is that constraints on OAR's may not be accurate, as the lack of soft tissue contrast in megavoltage conebeam CT (MV-CBCT) images may prevent delineation of structures such as the rectum and bladder. For example, changes in segment weighting may result in increased dose to the rectum. This may be overcome by creating and constraining the dose to a planning structure immediately posterior to the prostate. Likewise, a planning structure anterior to the prostate can be used to limit dose to the bladder.

This method has the potential to be implemented clinically as the aperture morphing technique works extremely quickly (less than 10 s followed by recalculation of the dose distribution). The main challenge is to enable efficient definition of the target volumes on the daily imaging. The lymph node structure can be transferred after performing rigid registration of the daily imaging data with the planning data set. The prostate volume can be defined using implanted

TABLE II. Change in dose in simulated treatment course.

Metric	No correction	Isoshift	Adapt morphing	Segment weight optimization
Prostate D95%	-1.6	3.8	5.4	4.9
Sem Ves D95%	-5.1	2.6	3.9	6.7
Lymph nodes D95%	-0.7	-5.3	-0.4	1.2

fiducial markers. Another challenge is the need to interact with the record and verify system to transfer the new fields from the planning system to the treatment machine on a daily basis. The objective from the original plan were used for re-optimization, thus saving time, but the segment weight optimization process still took approximately 4–5 min on a PC with a 3 GHz Intel[®] Xeon processor. Finally, recalculation of the treatment plan (and thus segment weight optimization) on the daily images requires image sets with (1) sufficient field of view and (2) calibrated density scaling. The second requirement can be fairly easily satisfied, but the requirement for sufficient FOV is not simply satisfied with our Siemens MV-CT imaging system. One potential solution is appropriately concatenating the planning CT and the MV-CT after image registration as shown in Fig. 6. However, this tool is not yet clinically available.

An alternative to using this method to adapt radiotherapy plans on a daily basis is to use aperture morphing to create multiple prostate plans for use with the multiple adaptive plan (MAP) strategy described by Xia *et al.*^{11,13,14} In the MAP strategy, multiple plans are created for each patient to accommodate different possible prostate locations. During treatment, one plan is chosen each day for delivery based on the prostate motion determined by daily imaging. One obstacle to the use of this strategy is the time required to produce multiple plans. Aperture morphing (with or without segment weight optimization) can overcome this obstacle because it can be used to efficiently create multiple plans.

There have been other adaptive strategies utilizing MLC leaf shifting reported in the literature. In particular, Ludlum *et al.* have also addressed the issue of treating the prostate and lymph nodes.¹⁵ Their proposal is to identify the MLC leaves that treat the prostate (as opposed to the nodes) and to shift the leaves as a function of the translational shift of the prostate relative to the nodes. The aperture morphing algorithm used in the Prowess system is a more general method, using not just the shift in the center of mass of the prostate, but potentially also changes in shape or rotations. Because it considers the projection of all targets in the BEV, it may also be more able to cope with potential overlaps between the pelvic lymph nodes, seminal vesicles, and the prostate, especially when used in conjunction with segment weight optimization. This is apparent when examining the results for the

seminal vesicles, which tended to be underdosed with aperture morphing alone (average change in D-95% = −4%). After segment weight optimization, the average change in D-95% for the seminal vesicles was less than 1%. Segment weight optimization may prove even more advantageous when using fractionation schemes with larger dose differences between the various targets (*e.g.*, 140 cGy and 200 cGy per fraction to the nodes and prostate, respectively). The study by Ludlum *et al.* does not report doses for the seminal vesicles. For a 1 cm posterior shift, they reported excellent results for prostate and lymph node coverage, with reductions of 1% or less using their leaf-shifting method. For 1 cm superior shifts, the prostate coverage (D-95%) was within 1% and the nodal coverage (D-95%) decreased by approximately 5%. Using the Prowess aperture morphing method, the mean reduction in D-95% for 1 cm shifts in any of four directions is 4% or less for the prostate, 6% or less for the seminal vesicles, and 4% or less for the lymph nodes. The segment weight re-optimization, as expected, improves the coverage of all target structures, with mean reductions of less than 2% for 1 cm shifts in any of the four directions considered.

In this study, the effectiveness of the aperture morphing and segment weight re-optimization method was tested for cases with various magnitudes of prostate shift, and was found to be effective for shifts as large as 1 cm. The dosimetric impact of using this adaptive method for a patient's treatment depends on the prostate motion for that particular patient over the treatment course. As an example, in this study the cumulative dose was calculated for a single patient using the daily prostate motion data acquired over 18 fractions. For this particular set of daily prostate shifts, the cumulative dose to the seminal vesicles and lymph node targets were decreased by 5% if no correction or the isoshift method is employed. Using adaptive morphing with or without segment weight re-optimization recovered full dose coverage of all targets. As with any adaptive method, however, there will be little benefit for patients who exhibit minimal prostate motion. The data in Figs. 3 and 4 suggest that for small shifts, 3 mm or less, it is probably unnecessary to perform any plan adaptation. Moreover, the cumulative dose may only be slightly affected for patients with large daily variations in prostate motion but whose average change in prostate position is close to zero (*i.e.*, minimal systematic error). As documented in the literature, prostate motion varies considerably between individuals.^{6,7} Generally the average prostate shift over the course of treatment is within 6 mm. For those individuals with average prostate shifts on the order of 6 mm, the data shown in Fig. 4 suggests that large decreases in lymph node coverage, in excess of 5%, can be prevented by using the proposed adaptive methods.

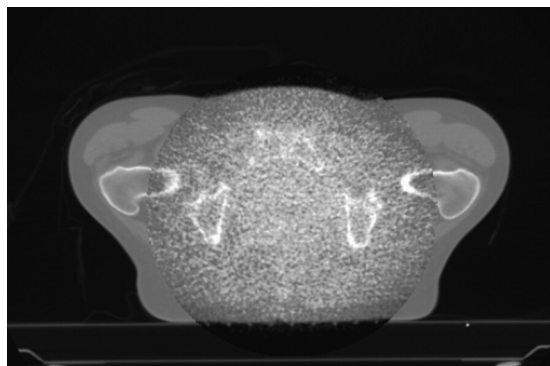


Fig. 6. Co-registered planning CT and MV-CT data sets can be concatenated to compensate for the limited field of view of the MV-CT image.

V. CONCLUSIONS

We have demonstrated that an algorithm using adaptive morphing with or without segment weight optimization can be used to compensate for the independent motion of the prostate and lymph nodes when combined with daily

imaging. This tool can be used alone or in conjunction with other strategies to compensate for the independent motion of the prostate and lymph nodes with, on average, less than 5% changes in the dose delivered to the target volumes.

ACKNOWLEDGMENTS

The authors want to thank Prowess, Inc. for their technical support and for providing the planning workstation. The authors also would like to thank Ping Xia for providing the daily prostate shift data.

^{a)}Author to whom correspondence should be addressed. Electronic mail: hwangab@gmail.com

¹M. Roach, 3rd, M. DeSilvio, C. Lawton, V. Uhl, M. Machtay, M. J. Seider, M. Rotman, C. Jones, S. O. Asbell, R. K. Valicenti, S. Han, C. R. Thomas, Jr., and W. S. Shipley, "Phase III trial comparing whole-pelvic versus prostate-only radiotherapy and neoadjuvant versus adjuvant combined androgen suppression: Radiation Therapy Oncology Group 9413," *J. Clin. Oncol.* **21**, 1904–1911 (2003).

²H. Lindsey, "Positive long-term outcomes for IMRT in prostate cancer," *Lancet Oncol.* **7**, 895 (2006).

³M. J. Zelefsky, H. Chan, M. Hunt, Y. Yamada, A. M. Shippey, and H. Amols, "Long-term outcome of high dose intensity modulated radiation therapy for patients with clinically localized prostate cancer," *J. Urol.* **176**, 1415–1419 (2006).

⁴M. Guckenberger, K. Baier, A. Richter, D. Vordermark, and M. Flentje, "Does intensity modulated radiation therapy (IMRT) prevent additional toxicity of treating the pelvic lymph nodes compared to treatment of the prostate only?," *Radiat. Oncol.* **3**, 3 (2008).

⁵A. Wang-Chesebro, P. Xia, J. Coleman, C. Akazawa, and M. Roach, 3rd, "Intensity-modulated radiotherapy improves lymph node coverage and dose to critical structures compared with three-dimensional conformal radiation therapy in clinically localized prostate cancer," *Int. J. Radiat. Oncol. Biol. Phys.* **66**, 654–662 (2006).

⁶K. M. Langen and D. T. Jones, "Organ motion and its management," *Int. J. Radiat. Oncol. Biol. Phys.* **50**, 265–278 (2001).

⁷K. C. Bylund, J. E. Bayouth, M. C. Smith, A. C. Hass, S. K. Bhatia, and J. M. Buatti, "Analysis of interfraction prostate motion using megavoltage cone beam computed tomography," *Int. J. Radiat. Oncol. Biol. Phys.* **72**, 949–956 (2008).

⁸W. Y. Song, E. Wong, G. S. Bauman, J. J. Battista, and J. Van Dyk, "Dosimetric evaluation of daily rigid and nonrigid geometric correction strategies during on-line image-guided radiation therapy (IGRT) of prostate cancer," *Med. Phys.* **34**, 352–365 (2007).

⁹H. A. Shih, M. Harisinghani, A. L. Zietman, J. A. Wolfgang, M. Saksena, and R. Weissleder, "Mapping of nodal disease in locally advanced prostate cancer: Rethinking the clinical target volume for pelvic nodal irradiation based on vascular rather than bony anatomy," *Int. J. Radiat. Oncol. Biol. Phys.* **63**, 1262–1269 (2005).

¹⁰E. E. Ahunbay, C. Peng, G. P. Chen, S. Narayanan, C. Yu, C. Lawton, and X. A. Li, "An on-line replanning scheme for interfractional variations," *Med. Phys.* **35**, 3607–3615 (2008).

¹¹P. Xia, P. Qi, A. Hwang, E. Kinsey, J. Pouliot, and M. Roach, 3rd, "Comparison of three strategies in management of independent movement of the prostate and pelvic lymph nodes," *Med. Phys.* **37**, 5006–5013 (2010).

¹²M. J. Zelefsky, D. Crean, G. S. Mageras, O. Lyass, L. Happersett, C. C. Ling, S. A. Leibel, Z. Fuks, S. Bull, H. M. Kooy, M. van Herk, and G. J. Kutcher, "Quantification and predictors of prostate position variability in 50 patients evaluated with multiple CT scans during conformal radiotherapy," *Radiother. Oncol.* **50**, 225–234 (1999).

¹³P. Xia, E. Ludlum, M. Aubin, J. Pouliot, A. Hwang, and M. Roach, 3rd, "Clinical validation of a novel adaptive approach for patients concurrently treated with the prostate and pelvic lymph nodes," *Med. Phys.* **35**, 2903 (2008).

¹⁴M. Roach, 3rd, J. Pouliot, and P. Xia, in *Image-Guided Radiation Therapy of Prostate Cancer*, edited by R. K. Valicenti, A. P. Dicker and D. A. Jaffray (Informa Healthcare, London, 2008), pp. 183–196.

¹⁵E. Ludlum, G. Mu, V. Weinberg, M. Roach, L. J. Verhey, and P. Xia, "An algorithm for shifting MLC shapes to adjust for daily prostate movement during concurrent treatment with pelvic lymph nodes," *Med. Phys.* **34**, 4750–4756 (2007).